



1 **Technical Note: Improved mathematical representation of** 2 **concentration-discharge relationships**

3

4 José Manuel Tunqui Neira^{1,2}, Vazken Andréassian¹, Gaëlle Tallec¹ & Jean-Marie Mouchel²

5 ⁽¹⁾ Irstea, HYCAR Research Unit, Antony, France

6 ⁽²⁾ Sorbonne University, UMR Metis 7619, Paris, France

7

8 **Abstract**

9 This Technical Note deals with the mathematical representation of concentration-discharge
10 relationships and with the identification of its parameters. We propose a two-sided power
11 transformation alternative to the classical log-log transformation, and a multicriterion identification
12 procedure allowing determining parameters that are efficient, both from the concentration and the
13 load points of view.

14 **Keywords**

15 Concentration-discharge relationships; log-log transformation; power transformation; multi-
16 objective calibration

17

18 **1. Introduction**

19 The relationship between ion concentrations and river discharge is an age-old topic in hydrology (see
20 among others Bazerbachi and Probst, 1986; Durum, 1953; Foster, 1978; Gibbs, 1970; Gregory and
21 Walling, 1973; Hem, 1948; Hendrickson and Krieger, 1960; Johnson et al., 1969; Meybeck, 1976).
22 Several recent articles (e.g. Bierozza et al., 2018; Chanat et al., 2002; Godsey et al., 2009; Meybeck and
23 Moatar, 2012; Moatar et al., 2017; Rose et al., 2018; Kirchner, 2019) give an exhaustive view of the
24 current work on this relationship. Since at least seventy years, a one-sided power relationship has
25 been used to represent and model this relationship (Eq. (1)).

26

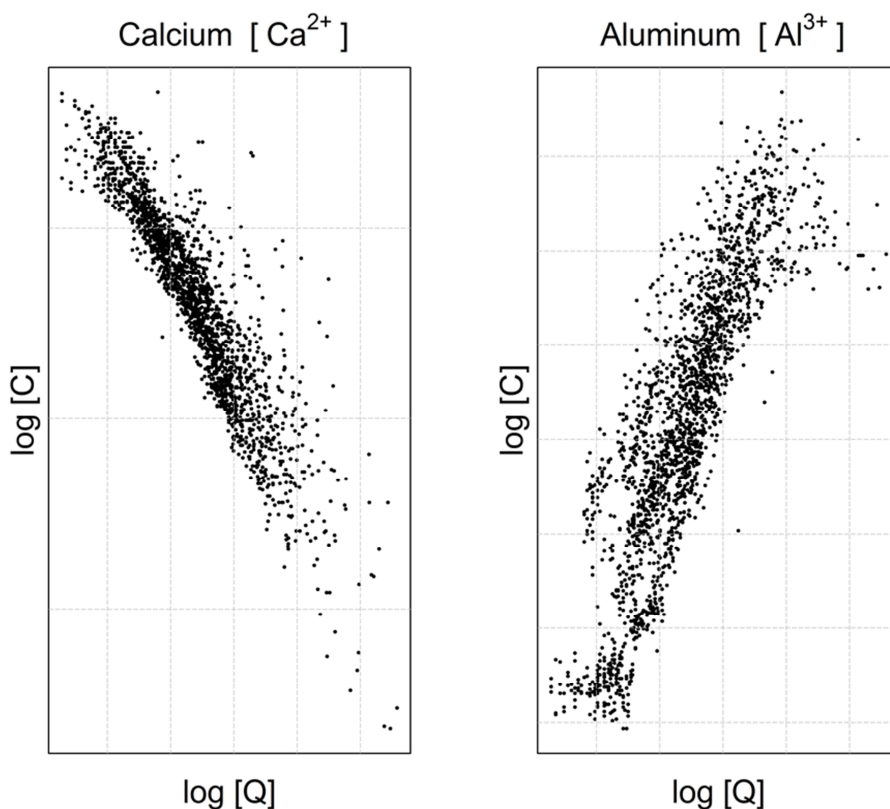
$$C = aQ^b \quad \text{Eq. (1)}$$

$$\ln(C) = \ln(a) + b \cdot \ln(Q) \quad \text{Eq. (2)}$$

27



28 From a graphical point of view, the one-sided power relation presented in Eq. (1) is equivalent to
29 plotting concentration and discharge in a log-log space, where parameters a and b can be identified
30 very simply, either graphically or numerically (under the classical assumptions of linear regression).
31 Obviously, not all ion species present a clear relationship between concentration and discharge; but
32 a few exhibit a very clear one as shown by the Figure 1 which gives an example from Upper Hafren
33 catchment data (Neal et al., 2013a; Neal et al., 2013b). In the rest of this note, we will focus explicitly
34 on the ions which exhibit a clear dependency between discharge and concentration.



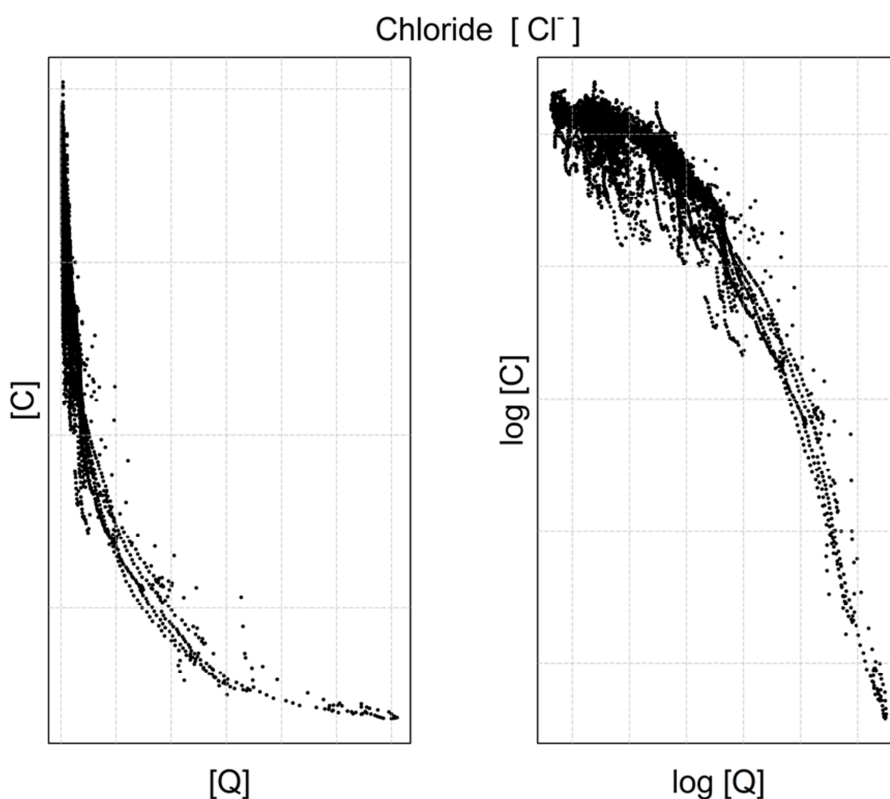
35
36 **Figure 1.** Illustration of the C-Q behavior of two ions (Calcium and Aluminum) showing a clear log-
37 log relationship. Data from Upper Hafren catchment, Wales, United Kingdom (Neal et al.,
38 2013a; Neal et al., 2013b)

40 2. About the “excess” of the log-log transformation

41 For many years, since the size of the C-Q datasets was limited by the cost of chemical analyses, it was
42 difficult to analyze in much detail the precise shape of the C-Q relationship. In many cases, the log-



43 log transformation appeared visually adequate (and conceptually simple), which explains its lasting
44 popularity. With the advent of high-frequency measuring devices in recent years, the size of the
45 datasets has exploded, and all the extremes of the relationship can now be included in the analysis.
46 Figure 2 shows an example from such a high-frequency dataset, collected from the Oracle-Orgeval
47 observatory (Tallec et al., 2015; Flourey et al., 2017). The 17500 data points represent half-hourly
48 measurements of ions collected over a two-year period, during which the catchment was exposed to
49 a variety of high- and low-flow events, which provides an unprecedented opportunity for exploring
50 the shape of the C-Q relationship.



51
52 **Figure 2. Concentration-discharge relationship observed on the Oracle-Orgeval observatory**
53 **(measurements from the “RiverLab”) for Chloride ions, with (right) and without (left) logarithm**
54 **transformation.**

55

56 Figure 2 illustrates what we call here the “excess” of the log-log transformation: the C-Q relationship
57 evolves from a clearly concave shape on the left to a slightly convex shape on the right. We have
58 gone beyond the straight shape that we aimed at. Note that this is not always the case, and the log-



59 log transformation can be well adapted in other situations (see Fig. 1 for the Upper Hafren data set
60 or further examples in the paper by Moatar et al., 2017). This slightly different shape may be due to
61 the high frequency of the time series (Moatar and Meybeck, 2007) or to catchment dynamics
62 (Kirchner, 2009), but in any case, it requires a different mathematical treatment than a logarithm
63 transformation.

64 **3. Box-Cox transformations as a continuous alternative to the log-log** 65 **transformations**

66 As a progressive alternative to the log-log transformation, we propose to use a two-sided power
67 transformation as shown in Eq. (3) (Box and Cox, 1964; Howarth and Earle, 1979).

$$C^{\frac{1}{n}} = a + bQ^{\frac{1}{n}} \quad \text{Eq. (3)}$$

68

69 The advantage of this transformation was already underlined by Box and Cox (1964): when n takes
70 high values, Eq. (3) converges towards the logarithm transformation (Eq. (2)), thus offering a
71 progressive solution. The reason is simple:

$$C^{\frac{1}{n}} = e^{\frac{1}{n} \ln C} \approx 1 + \frac{1}{n} \ln C \quad \text{when } n \text{ is large.}$$

72 Thus for large values of n , Eq. (3) can be written:

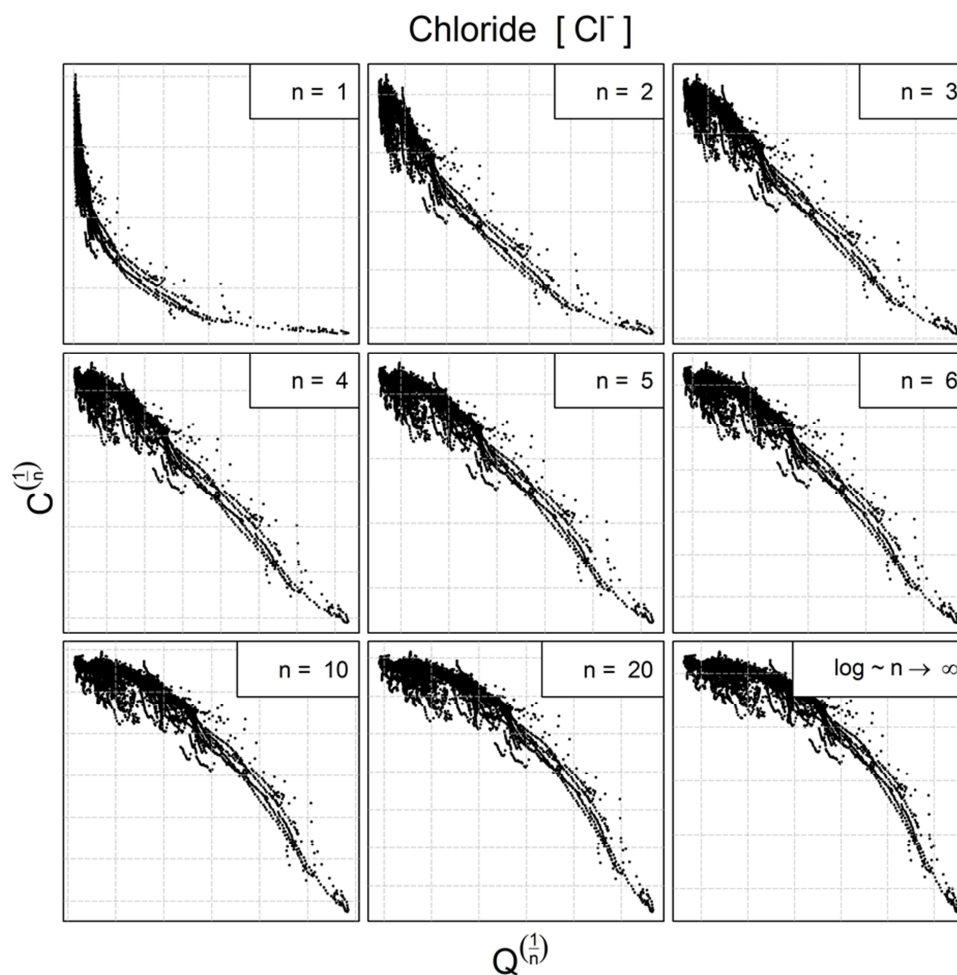
$$1 + \frac{1}{n} \ln C \approx a + b + \frac{b}{n} \ln Q$$

73 That is equivalent to

$$\ln C \approx A + b \ln Q \quad (\text{with } A = n(a + b - 1))$$

74 The progressive behavior and the convergence towards the log-log transformation are clearly
75 apparent in Figure 3.

76



77

78 **Figure 3.** Evolution of the shape of the concentration-discharge scatterplot with an increasing value
79 of n . Chloride ions concentrations measured on the Oracle-Orgeval observatory (“RiverLab”).

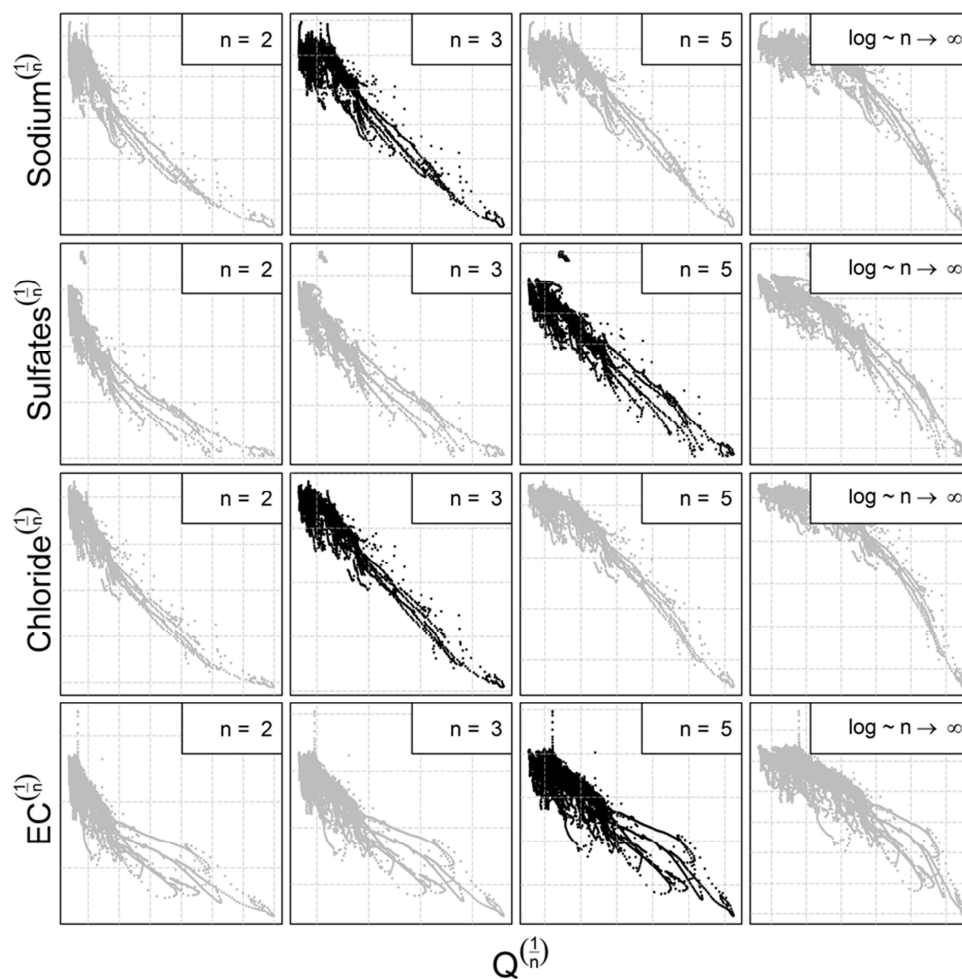
80

81 **4. Choosing an appropriate transformation for different ion species**

82 To our knowledge, there is no physical or mathematical reason why all ionic species should have a C-
83 Q relationship of the same shape. In Figure 4, we show the behavior of 3 ions and EC (Electrical
84 conductivity) from the same catchment and the same dataset (all four from the Oracle-Orgeval
85 observatory). The optimal shape could be chosen numerically (see Table 1), but we first followed the
86 advice of Box et al. (2016, p. 331) and did it visually. Figure 4 shows the most adapted power
87 transformation selected for each ion and EC.



88



89

90 **Figure 4: C-Q behavior of three different chemical species and the conductivity with different**
91 **transformations ($n = 2, 3, 5$ and \log). The optimal value of the power transformation (black dots)**
92 **has been chosen visually.**

93

94

95

96



97 **Table 1. Coefficient of determination (R^2) calculated for $n=1$ (no transformation), $n =$ optimal value
 98 **for two-sided power transformation (Figure 4) and $n \rightarrow \infty$ (log-log transformation) for each ion and**
 99 **for EC****

ion	n	R^2
Sodium	$n = 1$ (no transformation)	0.53
	$n = 3$ (optimal)	0.73
	$n \rightarrow \infty$ (log-log)	0.53
Sulfate	$n = 1$ (no transformation)	0.32
	$n = 5$ (optimal)	0.81
	$n \rightarrow \infty$ (log-log)	0.77
Chloride	$n = 1$ (no transformation)	0.52
	$n = 3$ (optimal)	0.88
	$n \rightarrow \infty$ (log-log)	0.69
EC	$n = 1$ (no transformation)	0.38
	$n = 5$ (optimal)	0.79
	$n \rightarrow \infty$ (log-log)	0.74

100

101 Although we indicated above that the value of n could be chosen visually, we have also calculated
 102 the coefficient of determination (R^2 see Table 1) to confirm our choice numerically. For each ion and
 103 EC, the n considered optimal has the highest R^2 value.

104 5. Multi-objective identification of the parameters of the C-Q relationship

105 Once the most appropriate value of the power transformation has been determined, the numerical
 106 identification of the optimal values of parameters a and b (see. Eq. (3)) should be easy. However, the
 107 extremely large number of values in the high-frequency dataset can prevent a robust identification
 108 over the full range of discharges, because the largest discharge values are in small numbers (in our
 109 dataset only 1% of discharges are in the range $[2.6 \text{ m}^3\text{s}^{-1}, 12.2 \text{ m}^3\text{s}^{-1}]$, and they correspond to the
 110 lowest concentrations (see Figure 2).

111 To avoid the difficulties linked with the overrepresentation of low-discharge / high-concentration
 112 data points, we tested successfully a multi-objective criterion for identifying the optimal couple (a,b) .
 113 We used an optimizing simultaneously on the quality of reproduction of the concentrations and the
 114 load (i.e. the discharge-weighted concentrations); otherwise, the large discharge-low concentration
 115 data points do not have enough weight to influence the selection of the parameter set.

116 The numerical criterion used for the concentration and the load is a bounded version of the Nash and
 117 Sutcliffe criterion (Mathevet et al., 2006). The Nash and Sutcliffe (1970) criterion (see Eq. (4) and Eq.
 118 (6), in Table 2) is well-known and widely used in the field of hydrology. The rescaling proposed by
 119 Mathevet et al. (2006) transforms NSE in NSEB, which varies between -1 and 1 (see Eq. (5) and Eq. (7)



120 in Table 2). The advantage of this rescaled version is to avoid the occurrence of large negative values
 121 (the original NSE criterion varies in the range $]-\infty, 1]$).

122 Last, we also used a combined criterion for both concentration and load, by averaging $NSEB_{conc}$ and
 123 $NSEB_{load}$ (see Eq. (8) in Table 2).

124

125 **Table 2. Numerical criteria used for optimization (C_{obs} – observed concentration, C_{cal} – computed
 126 concentration, Q – observed discharge)**

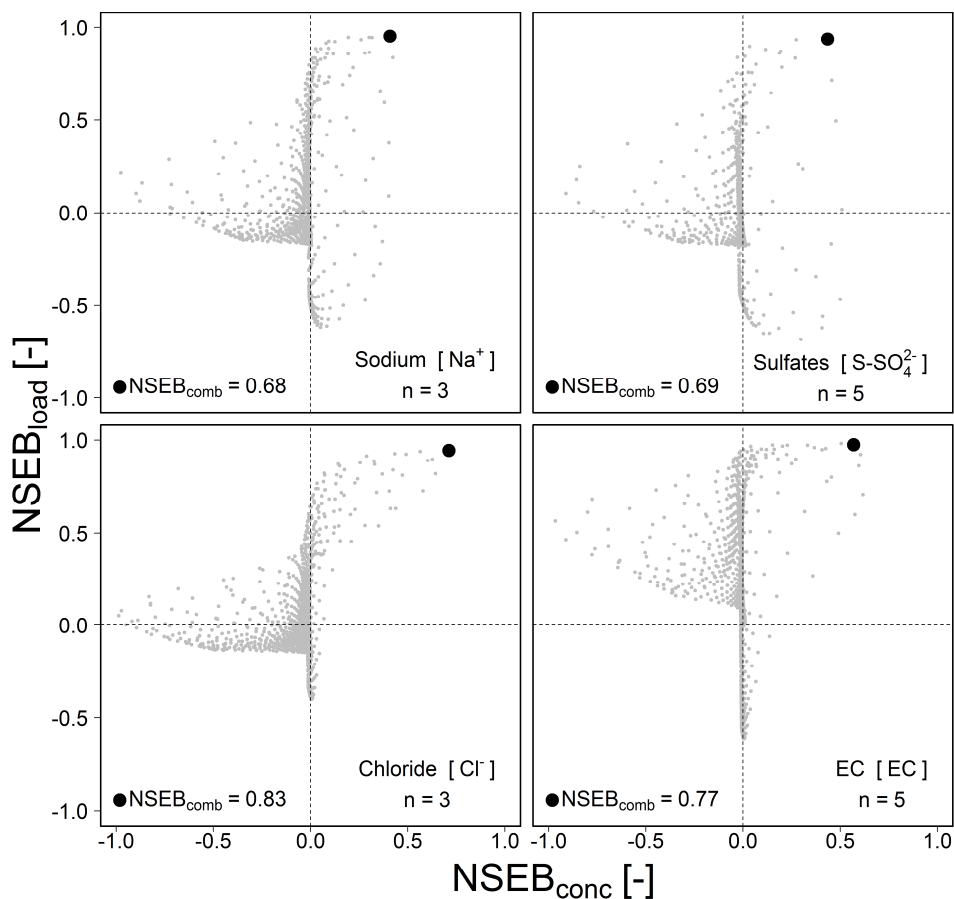
$NSE_{conc} = 1 - \frac{\sum_t (C_{obs}^t - C_{cal}^t)^2}{\sum_t (C_{obs}^t - \overline{C_{obs}})^2}$	Eq. (4)
$NSEB_{conc} = \frac{NSE_{conc}}{2 - NSE_{conc}}$	Eq. (5)
$NSE_{load} = 1 - \frac{\sum_t (Q^t C_{obs}^t - Q^t C_{cal}^t)^2}{\sum_t (Q^t C_{obs}^t - \overline{QC_{obs}})^2}$	Eq. (6)
$NSEB_{load} = \frac{NSE_{load}}{2 - NSE_{load}}$	Eq. (7)
$NSEB_{comb} = \frac{1}{2} (NSEB_{conc} + NSEB_{load})$	Eq. (8)

127

128 For the three ions and EC of the Oracle-Orgeval observatory, Figure 5 plots the performances of 6725
 129 random pairs of parameters a and b (see Eq. (3)). The Pareto plot allows us to visualize the best
 130 compromise between the criterion focusing on concentration ($NSEB_{conc}$) and the criterion focusing on
 131 load ($NSEB_{load}$). The black point in Figure 5 corresponds to the optimum identified by the combined
 132 criterion $NSEB_{comb}$.



133



134

135 **Figure 5. Multi-objective criterion $NSEB_{conc}$ vs $NSEB_{load}$ (Pareto plot) obtained from 3 chemical**
136 **species (Sodium, Sulfates, Chloride) and Electrical conductivity (EC) from the Oracle-Orgeval**
137 **observatory. The black points represent the performance of the pair having the best-combined**
138 **criterion $NSEB_{comb}$. Note that like NSE, the optimal value of NSEB is 1, and that a value of 0 shows a**
139 **very poor fit.**

140

141 The interest of the Pareto plot is clearly seen in Figure 5. Not all ion species and EC have the same
142 behavior: Chloride has a common optimum for the concentration and the load, while the others do
143 not: they benefit clearly from a compromise that can be either identified visually on the Pareto plot
144 or identified by the combined criterion $NSEB_{comb}$. The optimal $NSEB_{comb}$ criterion values for the three



145 ions and EC range from 0.68 to 0.83 (these values of NSEB correspond to “unbounded” NSE values
146 ranging from 0.77 to 0.91, which most hydrologists would consider very satisfying).

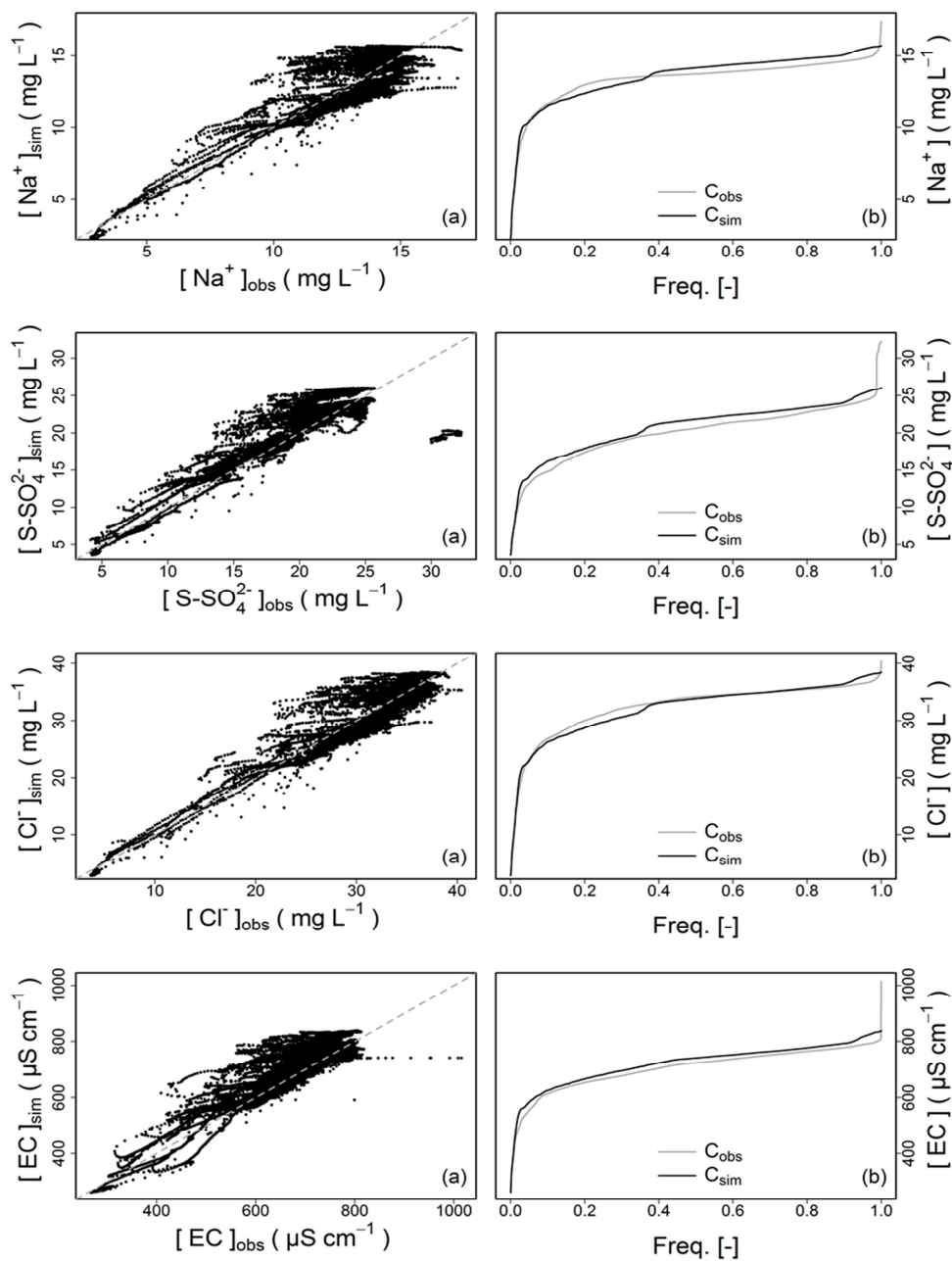
147 6. Results

148 The optimal values of a and b corresponding to the one shown on the Pareto plot (see Figure 5) and
149 the n value identified on Figure 4 are presented in Table 3, and Figure 6 illustrates the quality of the
150 fit over the entire calibration dataset (17500 points). Overall, the two-sided power transformation
151 model and the multicriterion identification procedure fit very well the concentrations. On can only
152 mention the difficulty of the model to reproduce the high extreme concentrations and conductivity
153 that would perhaps require a more elaborated model, which is out of the scope of this Technical
154 Note.

155

156 **Table 3. Summary of values a , b and n used to obtain the optimal $NSEB_{comb}$ criterion**

Ion	n	a	b	$NSEB_{comb}$
Sodium	3	-0.60	2.70	0.68
Sulfate	5	-0.55	2.20	0.69
Chloride	3	-1.00	3.70	0.83
EC	5	-0.70	4.20	0.77



157

158 **Figure 6. Comparison of observed concentrations with simulated concentrations by a two-sided**
159 **power transformation model: (a) Scatterplot between the observed and simulated concentration;**
160 **(b) Comparison of the cumulative frequency of the observed and simulated concentration.**

161



162 **7. Conclusion**

163 In this technical note, we discussed the log-log transformation, widely used by hydrologists to
164 represent concentration-discharge relationships, and showed that it is sometimes inadequate. The
165 two-sided power transformation we proposed is a valid and progressive alternative. We also showed
166 how the identification of the parameters of this relation can benefit of a multicriterion identification
167 procedure, combining efficiency in concentration and load representation. The simulated
168 concentrations for the 3 ions and the EC show a good performance.

169

170 *Data availability.* Data will be available in a dedicated database website after a contract accepted on
171 behalf of all institutes.

172

173 *Competing interests.* The authors declare that they have no conflict of interest.

174

175 *Acknowledgements.* The first author acknowledges the Peruvian Scholarship Cienciactiva of
176 CONCYTEC for supporting his Ph.D. Study at Irstea and the Sorbonne University. The authors
177 acknowledge the EQUIPEX CRITEX program (grant no. ANR-11-EQPX-0011) for the data availability.

178 **8. References**

179 Bazerbachi, A., and Probst, J.-L.: Transports en solution et en suspension par la Garonne supérieure.
180 *Solute and particulate transports by the upstream part of the Garonne river*, Sciences Géologiques,
181 bulletins et mémoires, 79-98, 1986.

182 Bierzoza, M. Z., Heathwaite, A. L., Bechmann, M., Kyllmar, K., and Jordan, P.: The concentration-
183 discharge slope as a tool for water quality management, *Science of The Total Environment*, 630, 738-
184 749, <https://doi.org/10.1016/j.scitotenv.2018.02.256>, 2018.

185 Box, G. E., and Cox, D. R.: An analysis of transformations, *Journal of the Royal Statistical Society:*
186 *Series B (Methodological)*, 26, 211-243, 1964.

187 Chanat, J. G., Rice, K. C., and Hornberger, G. M.: Consistency of patterns in concentration-discharge
188 plots, *Water Resources Research*, 38, 22-21-22-10, [10.1029/2001wr000971](https://doi.org/10.1029/2001wr000971), 2002.

189 Durum, W. H.: Relationship of the mineral constituents in solution to stream flow, Saline River near
190 Russell, Kansas, *Eos, Transactions American Geophysical Union*, 34, 435-442,
191 [10.1029/TR034i003p00435](https://doi.org/10.1029/TR034i003p00435), 1953.

192 Floury, P., Gaillardet, J., Gayer, E., Bouchez, J., Tallec, G., Ansart, P., Koch, F., Gorge, C., Blanchouin,
193 A., and Roubaty, J. L.: The potamochemical symphony: new progress in the high-frequency
194 acquisition of stream chemical data, *Hydrol. Earth Syst. Sci.*, 21, 6153-6165, 2017.

195 Foster, I. D. L.: Seasonal solute behaviour of stormflow in a small agricultural catchment, *CATENA*, 5,
196 151-163, [https://doi.org/10.1016/0341-8162\(78\)90006-1](https://doi.org/10.1016/0341-8162(78)90006-1), 1978.



- 197 Gibbs, R. J.: Mechanisms Controlling World Water Chemistry, *Science*, 170, 1088-1090,
198 10.1126/science.170.3962.1088, 1970.
- 199 Godsey, S. E., Kirchner, J. W., and Clow, D. W.: Concentration-discharge relationships reflect
200 chemostatic characteristics of US catchments, *Hydrological Processes*, 23, 1844-1864,
201 10.1002/hyp.7315, 2009.
- 202 Gregory, K. J., and Walling, D. E.: Quantitative evaluation of drainage basin process, in: *Drainage
203 basin form and process*, Fletcher & Son Ltd, United Kingdom, 184-225, 1973.
- 204 Hem, J. D.: Fluctuations in concentration of dissolved solids of some southwestern streams, *Eos,
205 Transactions American Geophysical Union*, 29, 80-84, 10.1029/TR029i001p00080, 1948.
- 206 Hendrickson, G., and Krieger, R.: Relationship of chemical quality of water to stream discharge in
207 Kentucky, *Proceedings of 21st International Geological Congress*, Norden, Denmark, 66-75, 1960.
- 208 Howarth, R., and Earle, S.: Application of a generalized power transformation to geochemical data,
209 *Journal of the International Association for Mathematical Geology*, 11, 45-62, 1979.
- 210 Johnson, N. M., Likens, G. E., Bormann, F. H., Fisher, D. W., and Pierce, R. S.: A working model for
211 variation in stream water chemistry at Hubbard-Brook-experimental-forest, new-hampshire, *Water
212 Resources Research*, 5, 1353-&, 10.1029/WR005i006p01353, 1969.
- 213 Kirchner, J. W.: Catchments as simple dynamical systems: Catchment characterization, rainfall-runoff
214 modeling, and doing hydrology backward, *Water Resources Research*, 45, 10.1029/2008wr006912,
215 2009.
- 216 Kirchner, J. W.: Quantifying new water fractions and transit time distributions using ensemble
217 hydrograph separation: theory and benchmark tests, *Hydrology & Earth System Sciences*, 23, 2019.
- 218 Mathevet, T., Michel, C., Andreassian, V., and Perrin, C.: A bounded version of the Nash-Sutcliffe
219 criterion for better model assessment on large sets of basins, *IAHS PUBLICATION*, 307, 211, 2006.
- 220 Meybeck, M.: Total mineral dissolved transport by world major rivers *Hydrological Sciences Bulletin*,
221 21, 265-284, 10.1080/02626667609491631, 1976.
- 222 Meybeck, M., and Moatar, F.: Daily variability of river concentrations and fluxes: indicators based on
223 the segmentation of the rating curve, *Hydrological Processes*, 26, 1188-1207, 2012.
- 224 Moatar, F., and Meybeck, M.: Riverine fluxes of pollutants: Towards predictions of uncertainties by
225 flux duration indicators, *Comptes Rendus Geoscience*, 339, 367-382,
226 <https://doi.org/10.1016/j.crte.2007.05.001>, 2007.
- 227 Moatar, F., Abbott, B., Minaudo, C., Curie, F., and Pinay, G.: Elemental properties, hydrology, and
228 biology interact to shape concentration-discharge curves for carbon, nutrients, sediment, and major
229 ions, *Water Resources Research*, 53, 1270-1287, 2017.
- 230 Nash, J. E., and Sutcliffe, J. V.: River flow forecasting through conceptual models part I—A discussion
231 of principles, *Journal of hydrology*, 10, 282-290, 1970.
- 232 Neal, C., Kirchner, J., and Reynolds, B.: Plynlimon research catchment high-frequency hydrochemistry
233 data. NERC Environmental Information Data Centre, 2013a.



234 Neal, C., Reynolds, B., Kirchner, J. W., Rowland, P., Norris, D., Sleep, D., Lawlor, A., Woods, C.,
235 Thacker, S., Guyatt, H., Vincent, C., Lehto, K., Grant, S., Williams, J., Neal, M., Wickham, H., Harman,
236 S., and Armstrong, L.: High-frequency precipitation and stream water quality time series from
237 Plynlimon, Wales: an openly accessible data resource spanning the periodic table, *Hydrological*
238 *Processes*, 27, 2531-2539, 2013b.

239 Rose, L. A., Karwan, D. L., and Godsey, S. E.: Concentration–discharge relationships describe solute
240 and sediment mobilization, reaction, and transport at event and longer timescales, *Hydrological*
241 *Processes*, 32, 2829-2844, 10.1002/hyp.13235, 2018.

242 Tallec, G., Ansard, P., Guérin, A., Delaigue, O., and Blanchoin, A.: Observatoire Oracle [Data set],
243 edited by: Irstea, <https://bdoh.irstea.fr/ORACLE/>, 2015.

244

245